

A Comprehensive Framework for Device-to-Device Communications in Cellular Networks

Xingqin Lin, Jeffrey G. Andrews and Amitava Ghosh

Abstract—Device-to-device (D2D) in cellular networks is a promising concept which opens up new opportunities for commercial applications but also brings new challenges for network management. In this paper, we propose a tractable hybrid network model where the positions of transceivers are modeled by random spatial Poisson point processes (PPP). Further, we develop a unified analytical approach which allows a unified capacity evaluation for different D2D deployment scenarios including overlay in-band D2D, underlay in-band D2D and out-of-band D2D. We further consider two important questions in the overlay case: 1) how to partition the spectrum between cellular and D2D transmissions, and 2) what is the optimal threshold for distance-based D2D mode selection? Similarly, we jointly study the optimal accessible spectrum fraction and mode selection threshold in the underlay case.

Index Terms—Device-to-device communication, cellular networks, spectrum sharing, mode selection, stochastic geometry.

I. INTRODUCTION

Device-to-device (D2D) networking allows direct communication between cellular users, thus bypassing the base stations (BS). D2D opens up new opportunities for commercial applications, such as proximity-based services, particularly social networking applications and local advertisement [1], [2]. Other use cases include public safety, local data transfer and data flooding [2]. Further, D2D opens up other potential benefits such as increased spectral efficiency, extended cellular coverage, improved energy efficiency and reduced backhaul demand [3], [4].

A. Related Work and Motivation

The idea of incorporating D2D communications in cellular networks, or more generally, the concept of hybrid network consisting of both infrastructure-based and ad hoc networks has long been a topic of considerable interest. In earlier studies D2D was mainly proposed for relaying purposes [5], [6]. By allowing radio signals to be relayed by mobiles in cellular networks, it was shown that the coverage and throughput performance can be improved [5], [6]. Meanwhile, researchers also studied ad hoc networks enhanced by infrastructure, particularly from the perspective of transport capacity [7]–[9]. Generally speaking, it has been shown that better scaling laws of transport capacity can be achieved in a hybrid network than in a *purely* ad hoc network.

Xingqin Lin and Jeffrey G. Andrews are with Department of Electrical & Computer Engineering, The University of Texas at Austin, USA. (E-mail: xlin@utexas.edu, jandrews@ece.utexas.edu). Amitava Ghosh is with Nokia Siemens Networks. (E-mail: amitava.ghosh@nsn.com). This research was supported by Nokia Siemens Networks.

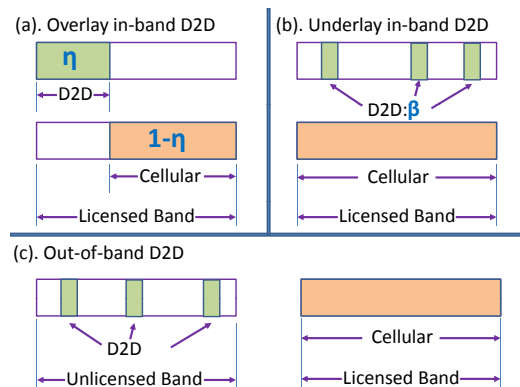


Fig. 1. Different D2D spectrum sharing scenarios

More recently, D2D in cellular networks has been motivated by the trend of proximity-based services [1], [2]; and thus Qualcomm publicized the necessity of developing tailored wireless technology to support D2D in cell phones and has also built a D2D demonstration system known as FlashLinQ [10], [11]. Now D2D is being studied and standardized by the 3rd Generation Partnership Project (3GPP). In particular, potential D2D use cases have been identified in [2]; and a new 3GPP study item focusing on the radio access aspect was agreed upon at the December 2012 RAN plenary meeting [12].

In parallel with the standardization effort in industry, basic research is being undertaken to address the many fundamental problems in supporting D2D in cellular networks; these problems can be broadly classified into two classes: device discovery and management of D2D links. Device discovery refers to the process of detecting surrounding devices and is the first step for D2D session setup [4], [11]. As for the management of D2D links, a first issue is how to share the spectrum resources between cellular communication and D2D communication; and based on the spectrum sharing manner, D2D can be classified into two types: *in-band* and *out-of-band*. In-band refers to the scenario that D2D uses the cellular spectrum. Conversely, out-of-band refers to the scenario that D2D utilizes different bands (e.g. 2.4GHz ISM band) other than the cellular band. In-band D2D can be further classified into two categories: *overlay* and *underlay*. Overlay means that cellular and D2D transmitters use orthogonal in-band spectrum, while underlay means that D2D transmitters opportunistically access spectrum that may be occupied by cellular users. These D2D scenarios are illustrated in Fig. 1.

Unlike the analysis and design of ad hoc networks which

are notoriously difficult (see e.g. [13]–[16]), D2D networking has certain conveniences; for example, D2D networking can be assisted by the cellular network infrastructure which is not available to ad hoc networks. Nevertheless, D2D networking introduces its own challenges. For example, the interference situation in the underlay in-band D2D case is more complicated than in a purely ad hoc network. Furthermore, supporting D2D communication requires the underlying cellular network to have a lot of new functionalities [2], [12]; this significantly complicates the cellular network design. To sum up, the analysis and design of cellular networks with D2D can be quite different from those of either ad hoc networks or traditional cellular networks. Thus, the objective of this paper is to provide an accurate but tractable baseline model for such D2D-enabled cellular networks. Further, we would like to develop a unified analytical framework for the corresponding performance analysis; this goal is fairly ambitious since the D2D scenarios are quite diverse.

In addition, with the proposed model and developed approach, we would like to show how they can be used for the design of D2D-enabled cellular networks, particularly those design questions shown in Fig. 1. Specifically, what is the proper spectrum fraction η that should be assigned to D2D communications? What is the proper spectrum fraction β that can be opportunistically accessed by underlaid D2D communications? These questions are largely open, though some preliminary results exist (see e.g. [17], [18]). The problems are further complicated by D2D *mode selection* which means that a potential D2D pair can switch between direct and conventional cellular communications. Determining an optimum D2D mode selection threshold – which we define as the Tx-Rx distance under which D2D communication should occur – is another objective of this paper.

B. Contributions and Outcomes

The main contributions and outcomes of this paper are as follows.

1) *A tractable hybrid network model*: In Section II, we introduce a tractable hybrid network model that captures many important characteristics of D2D mixed cellular networks including D2D mode selection, transmit power control and orthogonal scheduling of cellular users within a cell. We use Poisson point processes (PPP) [19] to model the spatial positions of the BSs, cellular and D2D transmitters. While such a random PPP model is well motivated by the random and unpredictable mobile user locations, the PPP model for BS locations has been recently shown to be about as accurate in terms of both SINR distribution and handover rate as the hexagonal grid for a representative urban cellular network [20], [21]. Surprisingly, as shown in Section VII, the performance gap between PPP and hexagonal models is found to be much smaller under the set-up in this paper; this finding further substantiates the plausibility of using random PPP model for assessing the statistical performance of cellular networks.

2) *A unified performance analysis approach*: In Section IV, we present a general analytical framework for system-wide performance evaluation in cellular networks. The proposed

model incorporates the impact of transmitter density, transmit power, power spectral density (PSD) and carrier frequency. Thus, compared to existing stochastic geometric models [20], [22], [23] (which usually include only first two factors), the new model provides a finer characterization on the received signal and interference, which may be most useful for studying out-of-band D2D where many heterogeneous interferers exist. Moreover, the developed approach provides a unified view on the impact of the received SINR on the performance (e.g., coverage, rate, moments of SINR, symbol or bit error rate) of communication systems with *arbitrary* signal and interference distributions. With this approach, a comprehensive but unified capacity evaluation and performance comparison are conducted for overlay and underlay in-band D2D; the analysis of out-of-band D2D is not included in this paper due to page limit.

3) *Design insights*: From the analytical results, several observations may be informative for system design. First, from the perspective of energy efficiency, the optimal D2D mode selection threshold is inversely proportional to the square root of BS density and monotonically increases with the path-loss exponent; moreover, it is invariant to the distance distribution of D2D pairs. Second, three design criteria - (weighted) max-sum, max-min and proportional fairness - are considered and optimal spectrum partition rules are derived in the overlay case. It is found that max-min and proportional fairness are appropriate metrics for spectrum partitioning; whereas max-sum yields a degenerative partition result (all or nothing). Third, in the underlay case, we reveal a tradeoff between the spectrum access factor and the D2D mode selection threshold: as more D2D links are allowed (due to a more relaxed mode selection threshold), the network should actually make *less* spectrum available to them, due to the interference caused to the cellular receivers.

Comparing the underlay and overlay scenarios, we see that while overlay results in higher per-link (average) spectral efficiency due to its orthogonalization of cellular and D2D links, underlay appears to achieve a higher actual throughput because the spectrum is more efficiently reused.¹ Finally, it is found that offloading by D2D with appropriate mode selection provides significant gain; for example, under certain parameters, numerical results show a $2\times$ network-wide average rate gain vs. pure cellular even if only 5% of the active communication links are underlay D2D links, due to their very high achieved rate.

II. SYSTEM MODEL AND PERFORMANCE METRICS

A. Network Model

We consider a hybrid network consisting of both cellular and D2D links and focus on the uplink system (see Fig. 2 for illustration²). The transmitting UEs are modeled by an

¹Utilizing interference cancellation or avoidance in the underlay scenario may recover the spectral efficiency loss (due to the mutual interference between cellular and D2D links) and further increase the overall advantage of underlay.

²This plot is just an illustration and does *not* exactly match the description of network model. In particular, the BS locations are deterministic in Fig. 2.

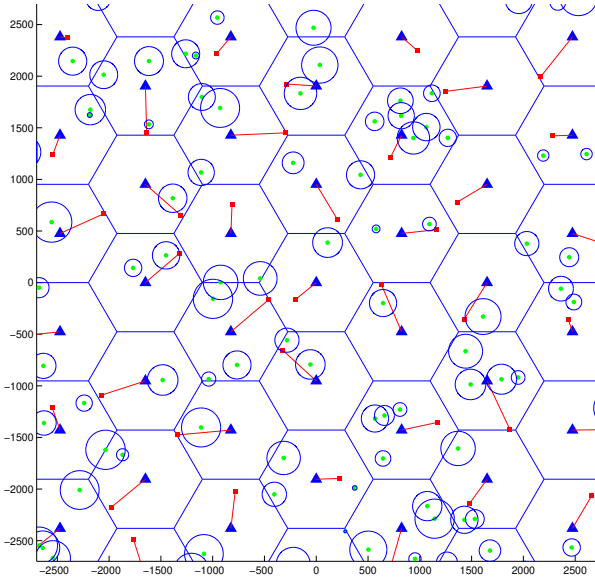


Fig. 2. A hybrid network consisting of both infrastructure-based cellular links and ad hoc D2D links. Blue solid triangles, red solid squares and green dots denote BSs, uplink cellular transmitters and D2D transmitters, respectively. For clarity we omit plotting D2D receivers, each of which is randomly located on the blue circle around its associated D2D transmitter.

independently marked Poisson point process (PPP) [20], [24] denoted as

$$\tilde{\Phi} = \{(X_i, \delta_i, L_i, P_i)\}.$$

Here $\{X_i\}$ denote the spatial locations of the UEs. Denote by $\Phi \in \mathbb{R}^2$ the unmarked PPP $\{X_i\}$ with λ being its intensity. $\{\delta_i\}$ denote the types of the UEs and are assumed to be i.i.d. Bernoulli random variables with $\mathbb{P}(\delta_i = 1) = q \in [0, 1]$. In particular, UE i is called a *Potential D2D UE*³ if $\delta_i = 1$; otherwise, it is called a *Cellular UE*. $\{L_i\}$ denote the lengths of radio links. Note that $\{L_i\}$ are not identically distributed. In particular, if $\delta_i = 1$, L_i represents the link length of Potential D2D UE i ; otherwise, L_i represents the cellular link length. So $\{L_i\}$ depend on $\{\delta_i\}$. Nevertheless, $\{L_i\}$ are still independent as each L_i only depends on δ_i and $\{\delta_i\}$ are independent. For notational simplicity, denote by L_d (resp. L_c) the generic random variable for $\{L_i\}$ with $\delta_i = 1$ (resp. $\delta_i = 0$). $\{P_i\}$ denote the transmit powers of UEs. In this paper we use channel inversion for power control, i.e., $P_i = L_i^\alpha$ where $\alpha > 2$ denotes the path-loss exponent; more sophisticated power control schemes are left to future work. It can be seen that $\{P_i\}$ are independent but not identically distributed. Similarly, we use P_d and P_c to denote the generic random variables for the transmit powers of Cellular and Potential D2D UEs, respectively.

For concreteness, we assume the transceiver distance D of a typical Potential D2D pair is Rayleigh distributed:

$$f_D(x) = 2\pi\lambda x e^{-\lambda\pi x^2}, \quad x \geq 0. \quad (1)$$

This Rayleigh distribution assumption is of practical interest

³It is called *Potential D2D UE* as a UE with D2D traffic can use either cellular or D2D mode.

[24]. Nevertheless, it is chosen here for exposition purpose and the following analysis can be extended to other distributions as well. Note that D is *not* the same as the previously defined D2D link length L_d ; $L_d = D$ only if the Potential D2D pair uses D2D mode. As for D2D mode selection: cellular mode is used if $D \geq \gamma_I$; otherwise, D2D mode is selected.

B. Transmission Scheduling

Cellular transmitters including Cellular UEs and Potential D2D UEs in cellular mode form a PPP Φ_c with intensity $\lambda_c = (1 - q)\lambda + q\lambda\mathbb{P}(D \geq \gamma_I)$. We assume an orthogonal multiple access technique and thus only one uplink transmitter in each macrocell can be active. Generally speaking, scheduling cellular transmitters in an orthogonal manner leads to *dependent thinning* of PPP Φ_c . This makes the analysis intractable and some simplified assumptions are needed (see e.g. [25]). In this paper, denoting by λ_b the density of BSs and \mathcal{A} the coverage region of a typical macrocell, we approximate \mathcal{A} by a disk with radius $R = \sqrt{\frac{1}{\pi\lambda_b}}$, i.e., $\mathcal{A} = \mathcal{B}(0, R)$ where $\mathcal{B}(x, r)$ denotes the ball centered at x with radius r . Further, we assume that the typical active cellular transmitter is uniformly distributed in the coverage region \mathcal{A} , and that the locations of the cellular interferers form a homogeneous PPP $\Phi_{c,a}$ with intensity λ_b , and interfering uplink signals come from those uplink interferers located outside the region \mathcal{A} .

Mathematically speaking, the above assumptions imply that the locations of uplink interferers form a *non-homogeneous* PPP with intensity measure $\lambda_b\mathbb{I}(\|x\| > R) dx$ where $x \in \mathbb{R}^2$ and $\mathbb{I}(\cdot)$ is the indicator function. This approximation will be validated in Section VII (see Fig. 4(a)). To avoid triviality, we assume $\lambda_c \geq \lambda_b$, which is reasonable as the uplink transmitter density is usually larger than BS density.

As for Potential D2D UEs in D2D mode, they form a PPP Φ_d with intensity $\lambda_d = q\lambda\mathbb{P}(D < \gamma_I)$. We assume that D2D transmitters are always active and leave D2D scheduling to future work.

C. Performance Metrics

We will analyze the average rates of Cellular and Potential D2D UEs, T_c and T_d . Note that

$$T_d = \mathbb{P}(D \geq \gamma_I) \cdot T_c + \mathbb{P}(D < \gamma_I) \cdot \hat{T}_d,$$

where \hat{T}_d denotes the average rate of Potential D2D UEs when in D2D mode. Clearly, T_c and T_d depend on the transmit power distributions of Cellular and Potential D2D UEs. Thus, we will also analyze the transmit power distributions, particularly $\mathbb{E}[P_c]$ and $\mathbb{E}[P_d]$, the average transmit powers of Cellular and Potential D2D UEs. Also note that

$$\mathbb{E}[P_d] = \mathbb{P}(D \geq \gamma_I) \cdot \mathbb{E}[P_c] + \mathbb{P}(D < \gamma_I) \cdot \mathbb{E}[\hat{P}_d],$$

where $\mathbb{E}[\hat{P}_d]$ denotes the average transmit powers of Potential D2D UEs in D2D mode.

III. TRANSMIT POWER ANALYSIS

In this section we analyze the average transmit powers of Cellular and Potential D2D UEs. This analysis is essential for rate analysis later.

Proposition 1. *The average transmit powers of a typical Cellular UE, a Potential D2D UE and a D2D mode UE are respectively given by*

$$\mathbb{E}[P_c] = \frac{1}{(1 + \frac{\alpha}{2})\pi^{\frac{\alpha}{2}}\lambda_b^{\frac{\alpha}{2}}} \quad (2)$$

$$\mathbb{E}[P_d] = e^{-\lambda\pi\gamma_I^2}\mathbb{E}[P_c] + \frac{\alpha}{2}(\lambda\pi)^{-\frac{\alpha}{2}}\gamma(\frac{\alpha}{2}, \lambda\pi\gamma_I^2) - \gamma_I^\alpha e^{-\lambda\pi\gamma_I^2}$$

$$\mathbb{E}[\hat{P}_d] = \frac{1}{1 - e^{-\lambda\pi\gamma_I^2}} \cdot \left(\frac{\alpha}{2}(\lambda\pi)^{-\frac{\alpha}{2}}\gamma(\frac{\alpha}{2}, \lambda\pi\gamma_I^2) - \gamma_I^\alpha e^{-\lambda\pi\gamma_I^2} \right),$$

where $\gamma(s, x) = \int_0^x z^{s-1}e^{-z} dz$ is the lower incomplete Gamma function.

Proof: See Appendix A. ■

We remark that the results presented in Prop. 1 are intuitive. When γ_I is small, using first order approximation $1 - e^{-x} \approx x$ and the following bounds

$$\Gamma(1 + \frac{\alpha}{2})(1 - e^{-(\Gamma(1 + \frac{\alpha}{2}))^{-\frac{2}{\alpha}}\lambda\pi\gamma_I^2})^{\frac{\alpha}{2}} \leq \frac{\alpha}{2}\gamma(\frac{\alpha}{2}, \lambda\pi\gamma_I^2) \leq \Gamma(1 + \frac{\alpha}{2})$$

we can see that $\mathbb{E}[\hat{P}_d] \approx \gamma_I^\alpha$, agreeing with intuition: $\mathbb{E}[\hat{P}_d]$ is proportional to γ_I^α and is approximately γ_I^α when γ_I is small. Further, both $\mathbb{E}[P_c]$ and $\mathbb{E}[P_d]$ increase as path-loss exponent α increases and are inversely proportional to the square root of BS density, which is natural.

Next let us examine the role of D2D mode selection threshold γ_I , which only affects $\mathbb{E}[P_d]$. As far as energy efficiency is concerned, one would like to choose γ_I such that $\mathbb{E}[P_d]$ is minimized.

Proposition 2. *For any PDF $f_D(x)$ of the random distance D , $\mathbb{E}[P_d]$ is minimized when*

$$\gamma_I^* = (\mathbb{E}[P_c])^{\frac{1}{\alpha}} = \left(\frac{1}{1 + \frac{\alpha}{2}} \right)^{\frac{1}{\alpha}} \cdot \sqrt{\frac{1}{\pi\lambda_b}}. \quad (3)$$

Proof: See Appendix B. ■

Prop. 2 shows that γ_I^* is only a function of the average transmit power $\mathbb{E}[P_c]$ of Cellular UEs and is independent of the distribution of D ; in particular, the Rayleigh assumption in (1) is not needed. Specifically, γ_I^* is inversely proportional to the square root of BS density λ_b , which is intuitive: cellular mode becomes more favorable when more BSs are available. In addition, $(\frac{1}{1 + \frac{\alpha}{2}})^{\frac{1}{\alpha}}$ monotonically increases as α increases. This implies that γ_I^* increases in α , agreeing with intuition: local transmission with D2D mode is more favorable for saving transmit power when the path loss-exponent increases.

Recall that the coverage of a typical BS is approximated as a disc with area $\pi R^2 = \frac{1}{\lambda_b}$. Hence, $\gamma_I^* = (\frac{1}{1 + \frac{\alpha}{2}})^{\frac{1}{\alpha}} \cdot R$. The largest $\gamma_{I,\max}^* = \lim_{\alpha \rightarrow \infty} \gamma_I^* = R$ and correspondingly the percentages of Potential D2D UEs using D2D mode equal $1 - e^{-1} = 63\%$. This gives an intuitive design insight: from the perspective of energy efficiency D2D mode is favorable only when the distance of a D2D pair is less than the coverage radius of a typical macrocell. The smallest $\gamma_{I,\min}^* = \lim_{\alpha \rightarrow 2} \gamma_I^* = 0.707R$. This implies that D2D mode is favorable even when the distance of a D2D pair exceeds two thirds of the coverage radius of a typical macrocell, which is a bit surprising. As a simple numerical example,

if $\alpha = 3$, $\lambda_b = \frac{1}{\pi 500^2}$, the optimal $\gamma_I^* = 354\text{m}$; accordingly, the percentages of Potential D2D UEs using cellular mode equal $e^{-\lambda\pi(\gamma_I^*)^2} = 61\%$. Finally, we stress that the ‘‘optimal’’ threshold given in Prop. 2 is optimal in the sense of energy efficiency, which is just one aspect of the network design.

IV. A UNIFIED ANALYTICAL APPROACH

In this section we describe a unified analytical approach which will be used to study overlay and underlay in-band D2D and out-of-band D2D in the next three sections.

A. A Generalized Channel Model

We first propose a generalized channel model. Consider a typical transmitter and receiver pair interfered by K types of heterogeneous interferers. The number of the k -th type interferers is denoted as M_k (which can be either deterministic or random); these interferers can differ in terms of density, carrier frequency, transmit power, power spectral density (PSD) and the supported modulation and coding scheme. The received signal at the typical receiver can be written as

$$Y_0(t) = \sqrt{P_0 L_0^{-\alpha}} H_0 S_0(t) + I_0(t) + Z_0(t), \quad (4)$$

where

$$I_0(t) = \sum_{k=1}^K \sum_{i=1}^{M_k} \sqrt{P_{k,i} R_{k,i}^{-\alpha}} H_{k,i} e^{j2\pi f_{k,i} t} S_{k,i}(t). \quad (5)$$

Here, P_0 , L_0 , H_0 and $S_0(t)$ are associated with the typical link and denote the typical link’s transmit power, length, channel fading and signal, respectively; $P_{k,i}$, $R_{k,i}$, $H_{k,i}$ and $S_{k,i}(t)$ are associated with the interfering link from transmitter i of type k to the typical receiver and denote the interfering link’s transmit power, length, channel fading and signal, respectively; the carrier frequency of $S_0(t)$ is shifted to 0 and $S_0(t)$ is assumed to be band-limited in the frequency range $(-\frac{1}{2}, \frac{1}{2})$, and correspondingly f_k represents the *relative* carrier frequency of the interferers of type k ; $Z_0(t)$ is additive white circularly symmetric Gaussian noise of power spectral density $\frac{N_0}{2}$ Watts/Hz. Further, denote by $\Phi_{k,i}(f)$ the PSD of random process $S_{k,i}(t)$ and assume $\int_{-\infty}^{\infty} \Phi_{k,i}(f) df = 1$, with a similar assumption for the PSD $\Phi_0(f)$ of $S_0(t)$.

Now assume the typical receiver uses an ideal low pass filter with cutoff frequency at $\pm\frac{1}{2}$. It follows that the signal power W , noise power σ^2 and interference power I are respectively given by $W = P_0 L_0^{-\alpha} \|H_0\|^2$, $\sigma^2 = \frac{N_0}{2}$, and

$$I = \sum_{k=1}^K \sum_{i=1}^{M_k} \varphi_k P_{k,i} R_{k,i}^{-\alpha} \|H_{k,i}\|^2,$$

where $\varphi_k = \int_{-1/2}^{1/2} \Phi_k(f - f_k) df$. The above three terms together determine the received SINR as

$$\text{SINR} = \frac{W}{I + N_0/2}.$$

In the proposed channel model (4), different carrier frequencies and PSDs are used to model the fact that signals of different transmitters may not fully overlap in the spectrum

(especially for wideband transmissions) and may use different types of physical layer technologies which necessarily lead to different PSDs. These facts are particularly true for out-of-band D2D, the study of which is not included in this paper due to page limit. In the sequel, we restrict the proposed channel model to just overlay and underlay in-band D2D study.

B. A Unified Approach to SINR-based Performance Metrics

The following lemma generalizes the result in [26] (where W is a Nakagami random variable with unit mean) and characterizes the impact of SINR in a unified way.

Lemma 1. *Suppose the following three conditions hold: (i) W is a nonnegative random variable whose pdf takes the form*

$$f_W(x) = \sum_{k \in \mathcal{K}} a_k f_{W_k}(x) = \sum_{k \in \mathcal{K}} a_k \frac{1}{\Gamma(k)\theta_k^k} x^{k-1} e^{-\frac{x}{\theta_k}}, x \geq 0,$$

where $\mathcal{K} \subset \mathbb{N}$ is any finite index set, $a_k \geq 0$ are weighted factors satisfying $\sum_{k \in \mathcal{K}} a_k = 1$, and $\theta_k > 0, \forall k \in \mathcal{K}$; (ii) the mapping $g: \mathbb{R}^+ \rightarrow \mathbb{R}$ is k^* times continuously differentiable where $k^* = \arg \max\{k: k \in \mathcal{K}\}$ and $g^{(i)}(0) < \infty, 0 \leq i \leq k^* - 1$; (iii) W and I are independent. Then, $\mathbb{E}[g(\text{SINR})]$ equals

$$\mathbb{E}\left[g\left(\frac{W}{I + N_0/2}\right)\right] = g(0) + \sum_{k \in \mathcal{K}} \frac{a_k \theta_k}{\Gamma(k) N_0/2} \int_0^\infty \left(\frac{d^k}{dz^k} z^{k-1} g(z)\right)_{z=\frac{\theta_k x}{N_0/2}} \cdot \mathcal{L}_I\left(\frac{x}{N_0/2}\right) e^{-x} dx, \quad (6)$$

where $\Gamma(z) = \int_0^\infty t^{z-1} e^{-t} dt$ is Gamma function and $\mathcal{L}_I(s) = \mathbb{E}[e^{-sI}]$ denotes the Laplace transform of I .

Proof: See Appendix C. ■

For a given $\mathbb{L}_I(s)$, (6) only involves one numerical integral and is very convenient for analytical purposes. Also, Lemma 1 is quite general. First, W can model a relatively large class of received signal powers in communication networks.

1) *Special case with $a_k = 1$ and for $\ell \neq k$, $a_\ell = 0$:* In this case, $f_W(x) = \frac{1}{\Gamma(k)\theta_k^k} x^{k-1} e^{-x/\theta_k}$ models Gamma distributed received power with mean $k\theta_k$, which is useful for multiple antenna techniques (see, e.g., [27]). When $k = 1$, $f_W(x) = \frac{1}{\theta_1} e^{-x/\theta_1}$ models exponentially distributed received power with mean θ_1 , a common single antenna model.

2) *Approximation for arbitrary distribution:* Let W_k be a Gamma random variable with shape k and scale θ_k , then $\mathbb{E}[W_k] = k\theta_k$ and $\text{Var}(W_k) = k\theta_k^2$. If we increase k while fixing $k\theta_k = \mu$ (where μ is any nonnegative constant), this yields a distribution with fixed mean μ and decreased variance as k increases. Hence, a weighted mixture $\sum_{k \in \mathcal{K}} a_k W_k$ of Gamma distributions with carefully chosen parameters can provide a good approximation for any discrete distribution, which in turn can be used to approximate a continuous distribution if desired.

Second, as pointed out in [26], the function $g(x)$ can represent many performance metrics in communication systems which are functions of received SINR. For example, 1) the achievable rate of a communication link can be calculated using $g(x) = \log(1+x)$; 2) the moments of SINR can be calculated using $g(x) = x^n, n = 1, 2, \dots$; 3) the (approximate) symbol or bit error rate and their bounds can be calculated

using $g(x) = Q(\sqrt{x})$ and e^{-x} . Lemma 1 can be used in all these examples. What we would like to emphasize is that even if the mapping g does not fully satisfy the conditions in Lemma 1, we can still use it in some cases by invoking appropriate approximation techniques. For example, consider the indicator mapping $g(x) = \mathbb{I}(x \geq \theta_{\text{th}})$ where θ_{th} is some SINR threshold for reliable detection. Then

$$\mathbb{E}[g(\text{SINR})] = \mathbb{E}[\mathbb{I}(\text{SINR} \geq \theta_{\text{th}})] = \mathbb{P}(\text{SINR} \geq \theta_{\text{th}}),$$

giving the complementary cumulative distribution function (CCDF) of SINR. Though the indicator mapping $g(x) = \mathbb{I}(x \geq \gamma_{\text{th}})$ is not continuously differentiable, we may choose the logistic function to approximate the indicator function as [28]

$$\mathbb{I}(x \geq \gamma_{\text{th}}) \approx \frac{1}{1 + e^{-c(x - \gamma_{\text{th}})}},$$

where $c > 0$ is a scaling constant. Using the proposed approximation, the CCDF of SINR can also be computed using Lemma 1.

Third, the assumption that signal power W and interference power I are independent is typical for tractable analysis in literature (see, e.g., [16], [23], [24]). In some cases, this assumption may not hold due for example to transmission scheduling, which introduces correlation between W and I . Nevertheless, Lemma 1 still can be used for approximate performance analysis, which usually yields a bound on the network performance.

In this paper, the following corollary will be particularly useful.

Corollary 1. *Suppose $\text{SINR} = \frac{W}{I + N_0/2}$ where $W \sim \text{Exp}(1)$ and I respectively denote the (random) signal and interference powers, and $N_0/2$ denotes the noise power. If W and I are independent,*

$$\mathbb{E}[\log(1 + \text{SINR})] = \int_0^\infty \frac{e^{-\frac{N_0}{2}x}}{1+x} \cdot \mathcal{L}_I(x) dx \quad (7)$$

$$\geq \sup_{s \geq 0} \log(1+s) e^{-\frac{N_0}{2}s} \mathcal{L}_I(s). \quad (8)$$

where $\mathcal{L}_I(s) = \mathbb{E}[e^{-sI}]$ denotes the Laplace transform of I .

Corollary 1 directly follows from Lemma 1. We also notice that the expression in (7) has been given in [24]. In this paper, the signal power is $W = PL^{-\alpha}G$ where G denotes the fading gain of the wireless link. Recall we assume channel inversion, i.e., $PL^{-\alpha} = 1$, and thus $W = G$. For simplicity we consider Rayleigh fading, i.e., $G \sim \text{Exp}(1)$, and assume independent fading over space. Thus, Corollary 1 can be directly applied in our setting.

V. ANALYSIS OF OVERLAY IN-BAND D2D

A. Link Spectral Efficiency

Let us consider a typical D2D link. With overlay in-band D2D, the interferers are D2D transmitters. The interference at the typical D2D receiver is given by

$$I_d = \sum_{X_i \in \Phi_d \setminus \{o\}} \hat{P}_{d,i} G_i \|X_i\|^{-\alpha},$$

where $G_i \sim \text{Exp}(1)$ denotes the fading from interferer X_i to the typical D2D receiver. Evaluating the Laplace transform of I_d and using Eq. (7) yields the following result.

Proposition 3. *With overlay in-band D2D, the spectral efficiency R_d of the D2D-mode link is given by*

$$R_d = \int_0^\infty \frac{e^{-\frac{N_0}{2}x}}{1+x} \cdot e^{-cx^{\frac{2}{\alpha}}} dx, \quad (9)$$

where c is a non-negative constant given by

$$c = \frac{q(1 - (1 + \lambda\pi\gamma_I^2)e^{-\lambda\pi\gamma_I^2})}{\text{sinc}(\frac{2}{\alpha})}. \quad (10)$$

Proof: See Appendix D. ■

Prop. 3 gives a clean characterization for the spectral efficiency R_d of the D2D link. We notice that as γ_I increases, c monotonically increases, which in turn results in monotonically decreasing R_d . This agrees with intuition: the spectral efficiency of per D2D link decreases when more Potential D2D UEs choose D2D mode (leading to increased interference).

Now let us consider a typical uplink. With overlay in-band D2D, the interferers are cellular transmitters in other cells. The interference at the typical BS is given by

$$I_c = \sum_{X_i \in \Phi_{c,d} \cap \mathcal{A}^c} P_{c,i} G_i \|X_i\|^{-\alpha}.$$

Evaluating the Laplace transform of I_c and using (7) yields the following result.

Proposition 4. *With overlay in-band D2D, the spectral efficiency R_c of the cellular link is given by*

$$R_c = \int_0^\infty \frac{e^{-\frac{N_0}{2}x}}{1+x} \cdot e^{-2\pi\lambda_b \int_R^\infty (1 - \mathbb{E}[e^{-xGL_c^\alpha r^{-\alpha}}])^r dr} dx, \quad (11)$$

where $R = \sqrt{\frac{1}{\pi\lambda_b}}$, L_c is distributed as $f_{L_c}(x) = 2\pi\lambda_b x \mathbb{I}(x \in [0, 1/\sqrt{\pi\lambda_b}])$, and $G \sim \text{Exp}(1)$.

B. Rates of Cellular and Potential D2D UEs

We are now in a position to derive the rates T_c and T_d . The throughput Q_c (bit/s/Hz) of a cellular link is the product of time resource $\frac{\lambda_b}{(1-q)\lambda + 2q\lambda e^{-\lambda\pi\gamma_I^2}}$ ⁴ (where recall $q\lambda e^{-\lambda\pi\gamma_I^2}$ is the density of Potential D2D UEs in cellular mode and the factor 2 accounts for the fact that 2 hops are needed per D2D flow in cellular mode) and cellular link spectral efficiency R_c . Mathematically,

$$Q_c = \frac{\lambda_b}{(1-q)\lambda + 2q\lambda e^{-\lambda\pi\gamma_I^2}} \cdot R_c. \quad (12)$$

The (normalized) average rate (bit/s) T_c of Cellular UEs thus equals Q_c multiplied by the available spectrum resource $1 - \eta$, i.e., $T_c = (1 - \eta)Q_c$.

In contrast, as no scheduling is assumed for D2D links, the throughput Q_d (bit/s/Hz) of a D2D link equals D2D link spectral efficiency R_d i.e., $Q_d = R_d$. Then the rate T_d

of Potential D2D UEs equals T_c if cellular mode is used; otherwise, i.e., D2D mode is used, it equals Q_d . Hence, $T_d = e^{-\lambda\pi\gamma_I^2}T_c + (1 - e^{-\lambda\pi\gamma_I^2})\eta Q_d$. Summarizing the above discussions yields the following Prop. 5.

Proposition 5. *With overlay in-band D2D, the (normalized) average rates (bit/s) of Cellular UEs and Potential D2D UEs, T_c and T_d , are given by*

$$\begin{aligned} T_c &= (1 - \eta)Q_c \\ T_d &= (1 - \eta)e^{-\lambda\pi\gamma_I^2}Q_c + \eta(1 - e^{-\lambda\pi\gamma_I^2})Q_d, \end{aligned} \quad (13)$$

where Q_c is given in (12) and $Q_d = R_d$.

C. Optimizing Spectrum Partition and Threshold Selection

In this section we study how to choose the optimal spectrum partition factor η^* such that

$$\eta^* = \arg \max_{\eta \in [0,1]} u(T_c, T_d).$$

where $u(x_1, x_2)$ is a utility function that can take different forms under different design metrics. In this paper we consider the following three popular design criteria: weighted max-sum $w_1x_1 + w_2x_2$, weighted max-min $\min(w_1x_1, w_2x_2)$, and weighted proportional fair $w_1 \log x_1 + w_2 \log x_2$. Here $w_1, w_2 > 0$ are weight factors such that $w_1 + w_2 = 1$.

Proposition 6. *The optimal weighted max-sum spectrum partition $\eta^* = 1$ if*

$$Q_d \geq \frac{w_d e^{-\lambda\pi\gamma_I^2} + w_c}{w_d(1 - e^{-\lambda\pi\gamma_I^2})} \cdot Q_c,$$

and $\eta^* = 0$ otherwise.

Proof: See Appendix E. ■

The partition rule in Prop. 6 is quite intuitive. Basically, it suggests that all the spectrum be assigned to the ‘‘dominated’’ transmission scheme (cellular or D2D) to maximize weighted sum rate. However, as the solution is degenerative, we do not pursue this partition rule in the sequel.

Proposition 7. *The optimal weighted proportional fair spectrum partition η^* is given by*

$$\eta^* = 1 - \frac{w_c}{w_c + w_d} \cdot \frac{1}{1 - (e^{\lambda\pi\gamma_I^2} - 1)^{-1} \frac{Q_c}{Q_d}}$$

if $Q_d > \frac{w_c + w_d}{w_d} \frac{1}{e^{\lambda\pi\gamma_I^2} - 1} Q_c$; otherwise, $\eta^* = 0$.

Proof: See Appendix F. ■

Note, if $\gamma_I \rightarrow \infty$, i.e., Potential D2D UEs are restricted to use D2D mode, $\lim_{\gamma_I \rightarrow \infty} \eta^* = \frac{w_d}{w_c + w_d}$ portion of the spectrum should be assigned to D2D transmissions to achieve proportional fairness.

Proposition 8. *The optimal weighted max-min spectrum partition η^* is given by*

$$\eta^* = \left(1 + \frac{1 - e^{-\lambda\pi\gamma_I^2}}{\frac{w_c}{w_d} - e^{-\lambda\pi\gamma_I^2}} \frac{Q_d}{Q_c} \right)^{-1}$$

if $Q_d > \frac{1}{e^{\lambda\pi\gamma_I^2} - 1} Q_c$ and $w_c > w_d e^{-\lambda\pi\gamma_I^2}$; otherwise, $\eta^* = 0$.

Proof: See Appendix G. ■

⁴For more accurate rate analysis, time resource should be multiplied by an extra constant factor 7/9 due to Feller’s paradox (see [29] for more details). We omit this constant as it does not affect the main results of this paper.

Note that the optimal spectrum partition factors η^* in Prop. 6, 7 and 8 are given for fixed D2D mode selection threshold γ_I . With $\eta^*(\gamma_I)$ we can further optimize the objective function $u(T_c, T_d)$ by choosing optimal γ_I^* . With the derived $\eta^*(\gamma_I)$ the objective function $u(T_c, T_d)$ is only a function of the scalar variable γ_I . Thus, the optimal γ_I^* can be found efficiently, and the computed $(\gamma_I^*, \eta^*(\gamma_I^*))$ gives the optimal system design choice.

VI. ANALYSIS OF UNDERLAY IN-BAND D2D

In the case of overlay in-band D2D, the analysis is restricted to narrowband transmissions. Analytical results for wideband transmissions can be readily obtained by appropriately scaling the narrowband results. In the case of underlay in-band D2D, it is more convenient to analyze wideband transmissions directly. Denoting by B the number of subchannels, D2D transmissions can access βB of them.

A. Link Spectral Efficiency

Let us consider a typical D2D link and denote by $\beta\Phi_d$ the PPP thinned from Φ_d with thinning probability β . With underlay in-band D2D, the interferers are thinned D2D transmitters excluding the typical link $\beta\Phi_d \setminus \{o\}$ of density $\beta q \lambda (1 - e^{-\lambda \pi \gamma_I^2})$ and cellular transmitters $\Phi_{c,a}$ of density λ_b . Using the channel model (4), the interference at the typical D2D receiver is given by

$$I_d = \sum_{X_i \in \beta\Phi_d \setminus \{o\}} \hat{P}_{d,i} G_i \|X_i\|^{-\alpha} + \sum_{X_i \in \Phi_{c,a}} P_{c,i} G_i \|X_i\|^{-\alpha},$$

Evaluating the Laplace transform of I_d and using (7) yields the following result.

Proposition 9. *With underlay in-band D2D, the spectral efficiency R_d of the D2D link is given by*

$$R_d = \int_0^\infty \frac{e^{-\frac{N_0}{2} \beta B x}}{1+x} \cdot e^{-c\beta x \frac{2}{\alpha}} \cdot e^{-\frac{1}{2\text{sinc}(\frac{2}{\alpha})}(\beta x) \frac{2}{\alpha}} dx. \quad (14)$$

Now let us consider a typical uplink. With underlay in-band D2D, the interferers are out-of-cell cellular transmitters $\Phi_{c,a} \cap \mathcal{A}^c$ and D2D transmitters in $\beta\Phi_d$. Using the channel model (4), the interference at the typical BS is given by

$$I_c = \sum_{X_i \in \Phi_{c,a} \cap \mathcal{A}^c} P_{c,i} G_i \|X_i\|^{-\alpha} + \sum_{X_i \in \beta\Phi_d} \hat{P}_{d,i} G_i \|X_i\|^{-\alpha}.$$

Using the independence of $\beta\Phi_d$ and $\Phi_{c,a} \cap \mathcal{A}^c$, Prop. 4 and 9, to calculate the Laplace transform of I_c , and further using (7) yields the following result.

Proposition 10. *With underlay in-band D2D, the spectral efficiency R_c of the cellular link is given by*

$$R_c = \int_0^\infty \frac{e^{-\frac{N_0}{2} B x}}{1+x} \cdot \mathcal{L}I_c(x) dx, \quad (15)$$

where

$$\mathcal{L}I_c(x) = e^{-c\beta^{1-\frac{2}{\alpha}} x \frac{2}{\alpha}} \cdot e^{-2\pi\lambda_b \int_R^\infty (1 - \mathbb{E}[e^{-xGL_c^\alpha r^{-\alpha}}]) r dr}.$$

Prop. 9 (resp. Prop. 10) implies that the spectral efficiency R_d of the D2D link (resp. R_c of the cellular link) decreases if β increases. In other words, with larger β , the increased D2D interferer density in each subchannel has a more significant impact than the decreased transmit power of D2D interferers. To sum up, from the perspective of maximizing the spectral efficiency of either D2D link or cellular link, the design insight here is that underlay in-band D2D should access less bandwidth with high power density rather than spreading power over more bandwidth. However, smaller β limits the spectrum resource available to D2D transmissions, which further limits the throughput/rate of D2D transmissions.

B. Tradeoff between Spectrum Access and Mode Selection

In this subsection, we take a closer look at Prop. 9 and 10 and show an interesting tradeoff between the spectrum access factor β and D2D mode selection threshold γ_I .

To begin with, suppose D2D transmissions have a target outage probability ϵ_d . Then D2D coverage probability (ignoring the noise) must satisfy

$$\begin{aligned} \mathbb{P}\left(\frac{W}{I_d} \geq \theta_d\right) &= \mathbb{E}[e^{-\beta B \theta_d I_d}] \geq 1 - \epsilon_d \\ \Rightarrow c(\gamma_I) \cdot \beta + \frac{1}{2\text{sinc}(\frac{2}{\alpha})} \cdot \beta^{\frac{2}{\alpha}} &\leq (\theta_d)^{-\frac{2}{\alpha}} \log\left(\frac{1}{1 - \epsilon_d}\right), \end{aligned} \quad (16)$$

where θ_d is the SIR threshold for successful D2D transmissions, and $c = c(\gamma_I)$ is given in Prop. 3 and monotonically increases as γ_I increases. Inequality (16) reveals the tradeoff between β and γ_I . In particular, if each D2D transmission has access to more spectrum, i.e. larger β , the signal power is spread in wider channel bandwidth and thus the effective SIR gets ‘‘thinner’’ in each subchannel. This in turn implies that with given quality-of-service (QoS) requirement θ_d and ϵ_d , less cochannel D2D transmissions can be supported, i.e., γ_I has to be decreased to make more Potential D2D UEs use cellular mode rather than D2D mode.

As in the case of D2D transmissions, if cellular transmissions have a target outage probability ϵ_c , the coverage probability (ignoring the noise) must satisfy

$$\begin{aligned} \mathbb{P}\left(\frac{W}{I_c} \geq \theta_c\right) &= \mathbb{E}[e^{-\theta_c I_c}] \geq 1 - \epsilon_c \\ \Rightarrow c(\gamma_I) \cdot \beta^{1-\frac{2}{\alpha}} &\leq \theta_c^{-\frac{2}{\alpha}} \cdot \\ &\left(\log\left(\frac{1}{1 - \epsilon_c}\right) - 2\pi\lambda_b \int_R^\infty (1 - \mathbb{E}[e^{-\theta_c GL_c^\alpha r^{-\alpha}}]) r dr\right), \end{aligned} \quad (17)$$

where θ_c is the SIR threshold for successful uplink transmissions. As in (16), inequality (17) imposes a joint constraint on β and γ_I ; a tradeoff between them exists.

We conclude this subsection with a numerical example given in Fig. 3 showing the tradeoff between β and γ_I . The blue and red curves respectively corresponding to the constraints (16) and (17) partition the first quadrant into four regions, of which the bottom one represents the feasible region of (γ_I, β) . Fig. 3 also indicates how the feasible region of (γ_I, β) will change if QoS parameters vary.

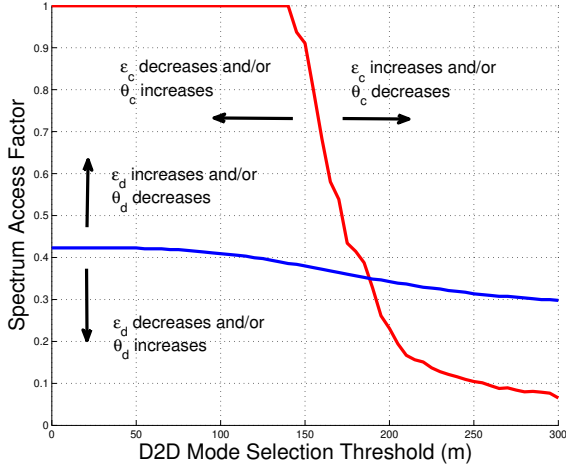


Fig. 3. Tradeoff between spectrum access factor β and D2D mode selection threshold γ_I . Here, $\theta_c = 0.1, \theta_d = 1, \epsilon_c = 0.05$ and $\epsilon_d = 0.4$; other parameters are specified in Table I.

C. Rates of Cellular and Potential D2D UEs

We are now in a position to derive the rates T_c and T_d . As in the case of overlay in-band D2D, the throughput Q_c (bit/s/Hz) of a cellular link is given by (12) with R_c replaced by the one in Prop. 10. The average rate (bit/s) T_c of Cellular UEs thus equals Q_c multiplied by the available spectrum resource B , i.e., $T_c = BQ_c$. In contrast, the throughput Q_d (bit/s/Hz) of a D2D link equals D2D link spectral efficiency R_d , i.e., $Q_d = R_d$. Then the rate T_d of Potential D2D UEs equals T_c if cellular mode is used; otherwise, it equals βBQ_d . Hence, $T_d = e^{-\lambda\pi\gamma_I^2}T_c + (1 - e^{-\lambda\pi\gamma_I^2})\beta BQ_d$. Summarizing the above yields the following Prop. 11.

Proposition 11. *With underlay in-band D2D, the average rates (bit/s) of Cellular UEs and Potential D2D UEs, T_c and T_d , are given by*

$$\begin{aligned} T_c &= BQ_c \\ T_d &= Be^{-\lambda\pi\gamma_I^2}Q_c + \beta B(1 - e^{-\lambda\pi\gamma_I^2})Q_d. \end{aligned} \quad (18)$$

To appreciate the difference between overlay and underlay, let $\eta = 0.5$ in Prop. 5, and $\beta = 1, B = 0.5$ in Prop. 11. Then the rates given in Prop. 5 have the same forms as their counterparts in Prop. 11. However, the underlay spectral efficiencies in Prop. 11 are worse than those in Prop. 5, whereas underlay consumes less spectrum ($B = 0.5$) than overlay ($2\eta = 1$).

As in the case of overlay, we choose an optimal spectrum access factor β^* in underlay such that

$$\beta^* = \arg \max_{\eta \in [0,1]} u(T_c, T_d).$$

However, a closed form solution for β^* is hard to obtain as β in underlay has a much more complicated impact on T_c (resp. T_d) than η in overlay. Instead, we report some numerical examples in Section VII.

Density of macrocells λ_b	$(\pi 500^2)^{-1}$
Density of UEs λ	$10 \times (\pi 500^2)^{-1}$
Portion of Potential D2D UEs q	0.2
Path loss exponent α	3
D2D mode selection threshold γ_I	200m
Spectrum partition factor η	0.2
UE weights (w_c, w_d)	(0.6, 0.4)
Spectrum access factor β	1
Number of subchannels B	1

TABLE I
SIMULATION/NUMERICAL PARAMETERS

VII. NUMERICAL RESULTS AND DISCUSSIONS

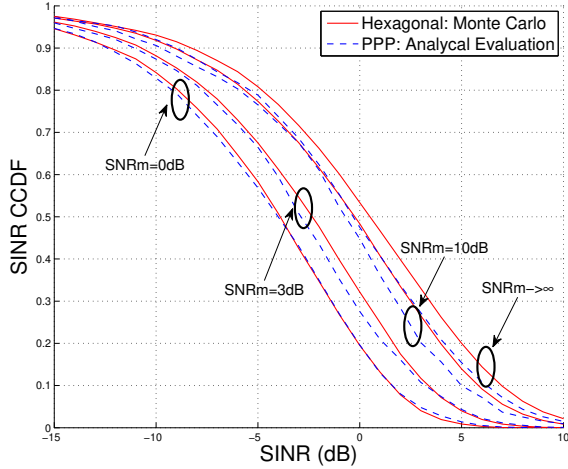
In this section we provide some numerical results to demonstrate the analytical results. The specific parameters used are summarized in Table I unless otherwise specified. Another notation we use in this section is SNR_m which equals the average *received* signal power normalized by noise power. Note that for ease of exposition, we assume in the analysis that the average received power is 1 due to channel inversion. However, the average received power can still be tuned by controlling the extent to which channel is inverted; this leads to different SNR_m values. Numerically, this can be achieved by “artificially” varying the noise power.

A. Validation of Analytical Results

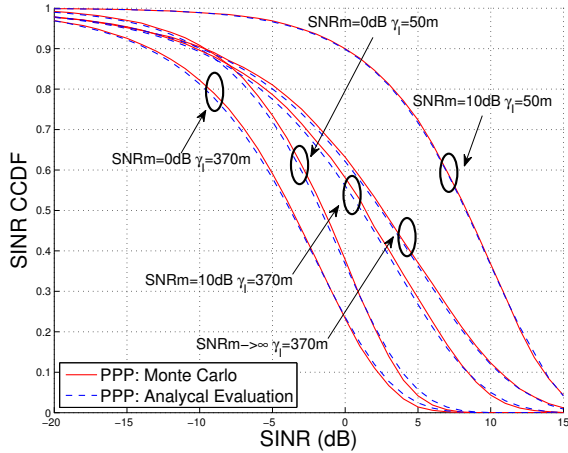
First we validate the analytical results. As all of the analytical results presented in this paper are functions of SINR. It suffices to validate the analytical SINR distributions by simulations rather than repetitively validating each analytical expression which in turn is a function of SINR. We compare uplink SINR CCDF (which can be inferred from Prop. 3) to the corresponding empirical distribution obtained from the classic hexagonal model. The center cell is treated as the typical one, while the remaining cells act as interfering cells. Each active uplink transmitter is uniformly distributed in its associated hexagonal cell. Fig. 4(a) plots the results, showing that the analytical results match the empirical results fairly well; the small gaps arise as we approximate the hexagonal model using a PPP model with a guard radius. We next compare the SINR distribution of a typical D2D link (which can be inferred from Prop. 2) to the corresponding empirical distribution obtained from Monte Carlo simulations. The results are shown in Fig. 4(b), from which we can see that the analytical results closely match the empirical results.

B. Overlay In-band D2D

In this part we provide some numerical results for underlay in-band D2D. We first show in Fig. 5 the average rates of Cellular and Potential D2D UEs as a function of D2D mode selection threshold γ_I . As expected, the average rate of Cellular UEs increases as γ_I increases as less Potential D2D UEs choose cellular model and correspondingly Cellular UEs can be scheduled more often. In contrast, the average rate of Potential D2D UEs first increases and then decreases



(a)



(b)

Fig. 4. Validation of the analytical SINR CCDF of cellular and D2D links.

as γ_I increases. This is because the average rate of Potential D2D UEs is co-determined by its cellular-mode rate and D2D-mode rate; cellular-mode rate increases in γ_I while D2D-mode rate decreases in γ_I (due to the increased intra-tier interference). Fig. 5 further shows that offloading by D2D with appropriate mode selection provides significant gain. Take $\text{SNR}_m = 10\text{dB}$ for example. Without supporting D2D (i.e., $\gamma_I = 0\text{m}$), the (normalized) sum rate equals 0.05; whereas in the case of D2D with $\gamma_I = 200\text{m}$, the sum rate equals $0.066 \times (1 - q) + 0.225 \times q = 0.0978$. Thus, an almost $2 \times$ gain is achieved, unequivocally demonstrating the merits of localizing communications via D2D.

We next show the optimal spectrum partition η^* under weighted proportional fair criterion in Fig. 6. As shown in Fig. 6(b), γ_I^* (with optimal η^*) roughly ranges from 250m to 400m as the portion of Potential D2D UEs q ranges from 0.1 to 0.9, and it increases as q increases, agreeing with intuition: D2D mode should be more aggressively used when there are more D2D traffic. Further, Fig. 6(a) shows that η^* converges to $\frac{w_d}{w_c + w_d} = 0.4$ very fast as γ_I increases. Recall that Prop. 2 gives $\gamma_I = 354\text{m}$ (under the current numerical setup) which

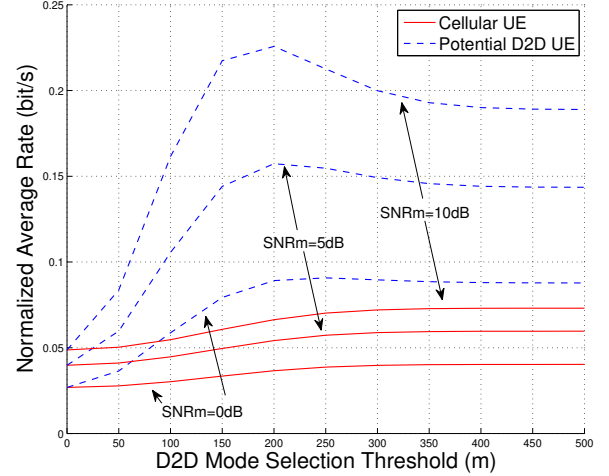


Fig. 5. Average rates of Cellular and Potential D2D UEs in the case of overlay in-band D2D.

minimizes UE transmit power. These facts together suggest the following rule of thumb

$$(\eta^\dagger, \gamma_I^\dagger) = \left(\frac{w_d}{w_c + w_d}, \left(\frac{1}{1 + \frac{\alpha}{2}} \right)^{\frac{1}{\alpha}} \cdot \sqrt{\frac{1}{\pi \lambda_b}} \right)$$

for spectrum partition and mode selection in D2D overlaid cellular networks with proportional fairness.

Similar plots for the optimal η^* under weighted max-min criterion are omitted due to page limit; instead, we briefly summarize the observations here. As in the proportional fair case, γ_I^* roughly ranges from 250m to 400m as q ranges from 0.1 to 0.9, and it increases as q increases. Nevertheless, with optimal γ_I^* max-min criterion tends to allocate much more spectrum than proportional fair criterion: max-min $\eta^*(\gamma_I^*)$ roughly increases linearly while proportional fair $\eta^*(\gamma_I^*)$ converges to $\frac{w_d}{w_c + w_d}$. For spectrum partition and mode selection in D2D overlaid cellular networks with max-min fairness, we can consider the rule of thumb

$$(\eta^\dagger, \gamma_I^\dagger) = \left(\eta_{\max - \min}^*, \left(\frac{1}{1 + \frac{\alpha}{2}} \right)^{\frac{1}{\alpha}} \cdot \sqrt{\frac{1}{\pi \lambda_b}} \right),$$

where $\eta_{\max - \min}^*$ is given in Prop. 8 (with γ_I replaced by $(\frac{1}{1 + \frac{\alpha}{2}})^{\frac{1}{\alpha}} \cdot \sqrt{\frac{1}{\pi \lambda_b}}$).

C. Underlay In-band D2D

In this part we provide some numerical results for underlay in-band D2D. We first show in Fig. 7 the average rates of Cellular and Potential D2D UEs as a function of γ_I . Compared to overlay, the average rate of Cellular UEs is less sensitive with respect to γ_I , which is due to the two competing effects below: increasing γ_I makes more Potential D2D UEs use D2D mode and correspondingly Cellular UEs can be scheduled more often by the BSs; however, more Potential D2D UEs using D2D mode in turn leads to increased inter-tier interference to cellular transmissions. Fig. 7 also shows the offloading gain of D2D underlay; for example, a $2 \times$ gain

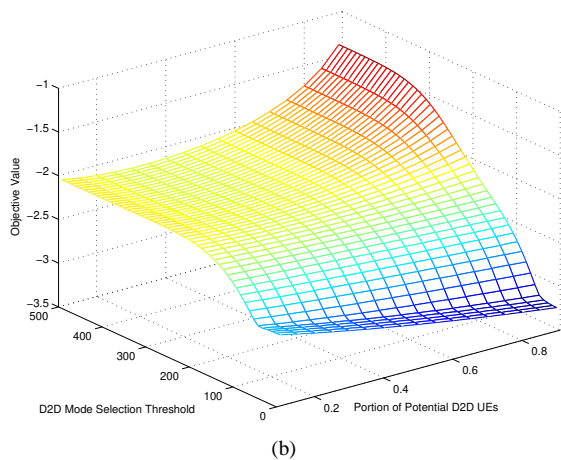
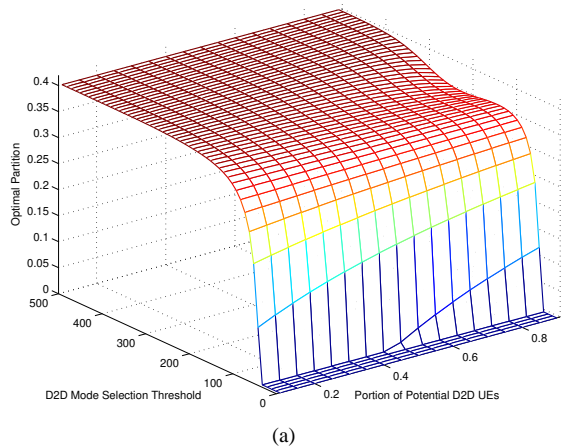


Fig. 6. Optimal weighted *proportional fair* η^* as a function of γ_I and q . Fig. 6(b) plots the corresponding objective value under η^* .

is achieved in the case of $\text{SNR}_m = 10\text{dB}$ and $\beta = 1$ with $\gamma_I = 250\text{m}$.

We next show some numerical values for the optimal spectrum access factor and D2D mode selection threshold (β^*, γ_I^*) in Table II; the results are obtained by searching over $\beta \in [0, 1, 1]$ and $\gamma_I \in [0, 500\text{m}]$ while ignoring the QoS constraints (16) and (17). First, we observe the optimal values (β^*, γ_I^*) with $\alpha = 3$ are quite close to their counterparts with $\alpha = 4$; this shows that (β^*, γ_I^*) is relatively invariant in α . Second, max-sum and proportional fair criteria yield similar (β^*, γ_I^*) ; whereas max-min criterion gives quite different results. Specifically, in the case $(q, \alpha) = (0.1, 3)$, the interference from underlaid D2D links is not severe; and the max-sum (resp. proportional fair) criterion aggressively favors the rates of potential D2D UEs by allowing the underlaid D2D links to access a large fraction of the spectrum. In contrast, with $(q, \alpha) = (0.9, 3)$, the interference from underlaid D2D links severely hurts (both cellular and D2D) link spectral efficiency; thus the max-sum (resp. proportional fair) criterion restricts the underlaid D2D links to access a small fraction of the spectrum to protect the link spectral efficiency. Nevertheless, the max-sum (resp. proportional fair) criterion still tries to take advantage of the gains of D2D links by increasing the mode

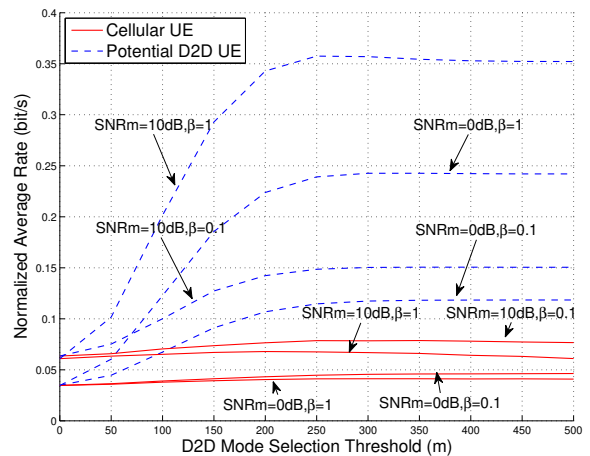


Fig. 7. Average rates of Cellular and Potential D2D UEs in the case of underlay in-band D2D.

(q, α)	Max-Sum	Proportional Fair	Max-Min
(0.1, 3)	(1.0, 350)	(0.9, 400)	(0.1, 470)
(0.9, 3)	(0.1, 470)	(0.2, 460)	(0.8, 270)
(0.1, 4)	(1.0, 400)	(1.0, 400)	(0.1, 450)
(0.9, 4)	(0.1, 500)	(0.2, 480)	(0.7, 260)

TABLE II
OPTIMAL SPECTRUM ACCESS FACTOR AND D2D MODE SELECTION THRESHOLD (β^*, γ_I^*) UNDER $\text{SNR}_m = 0\text{ dB}$.

selection threshold γ_I from 350m to 470m (resp. from 400m to 460m).

As for the max-min criterion, with $(q, \alpha) = (0.1, 3)$, the bottleneck is the rate of cellular UEs; thus the underlaid D2D links should only access a small fraction of the spectrum to limit their impact on cellular UEs. In contrast, with $(q, \alpha) = (0.9, 3)$, the rate of Potential D2D UEs becomes the bottleneck. Correspondingly, the underlaid D2D links should access a large fraction of the spectrum to increase their rate. Meanwhile, the mode selection threshold decreases from 470m to 270m in order to alleviate the interference caused by D2D links.

D. System Design Discussion

Thus far, we have ignored the discovery process that is required to pair D2D transmitters and receivers. In our results, therefore, D2D communication is generally preferred if the direct hop is better than going through two “hops” using the base station (in terms of network-wide impact). In practice, the D2D discovery and pairing process can incur significant overhead, and BS assistance is necessary to keep such overhead manageable. In this section, we discuss how the BSs can help exercise control in the proposed overlay and underlay models.

In the **overlay case**, relatively relaxed network control over D2D communications appears to be sufficient, since the D2D communication occurs in a parallel channel and thus is more independent of the conventional cellular network. Specifically, the network can use the derived spectrum partition rules (cf.

Section V-C) to find the appropriate spectrum resource portion η and mode selection threshold γ_I . These values can be shared with the UEs in a semi-static manner since they change very slowly, due to the lack of interference between the D2D and cellular networks. Then on a much shorter time scale each D2D pair can autonomously decide its own transmission attributes such as modulation scheme, transmit power and use of hybrid automatic repeat reques (HARQ). While cellular transmissions continue to be centrally scheduled by the BSs, the D2D access mechanism is presumably distributed and likely some form of random access should be used. Because the mode selection depends on the states in both the D2D and cellular network, we suggest that the BS retain control of whether UEs in its cell operate in D2D or cellular mode.

In the **underlay case**, tighter network control over the D2D communications is needed because of the interference coupling between the D2D transmitters and the cellular receivers. Specifically, the network has to tune optimal spectrum access factor β and mode selection threshold γ_I in a much more dynamic manner to keep link outage within an acceptable level (e.g. so that both (16) and (17) are satisfied). Also, now the network may wish to control other aspects of D2D communications including its access mechanism, link adaptation and use of HARQ, as well as the mode selection. Although both cellular and D2D links may be scheduled by the BSs, cellular links are scheduled on a fine time scale (e.g. 1ms in LTE); scheduling underlaid D2D links on such a short time scale may result in unnecessarily large control signaling overhead (both in the reporting of channel quality indicator (CQI) and the assignment of resources). Thus, we suggest that underlaid D2D communications be scheduled on relatively longer time scale (e.g. 10-100ms), in a semi-persistent manner.

VIII. CONCLUSIONS

This paper presents a general analytical framework for system-wide performance evaluation in cellular networks. The proposed framework has been applied to capacity evaluation and system design of overlay and underlay in-band D2D. The ground cellular network studied is of traditional cellular architecture consisting of only tower-mounted macro BSs. It is interesting to extend this work to (possibly multi-band) heterogeneous networks [29], [30] consisting of different types of lower power nodes besides macro BSs.

This work can be further extended in a number of ways. At the PHY layer, it would be of particular interest to extend the currently investigated point-to-point D2D communications to group communication and broadcasting as they are important D2D use cases. It is also desirable to study the impact of multiple antenna techniques. At the MAC layer, it would be useful to explore efficient D2D scheduling mechanisms. At the network layer, our work can be used as a stepstone for a wide range of interesting topics including multi-hop and cooperative D2D communications.

APPENDIX

A. Proof of Proposition 1

For cellular link, the pdf of the link length is

$$f_{L_c}(x) = \begin{cases} 2\pi\lambda_b \cdot x & \text{if } x \in [0, 1/\sqrt{\pi\lambda_b}]; \\ 0 & \text{otherwise.} \end{cases}$$

The average transmit power of a cellular transmitter is

$$\begin{aligned} \mathbb{E}[P_c] &= \mathbb{E}[L_c^\alpha] = \int_0^{1/\sqrt{\pi\lambda_b}} 2\pi\lambda_b x^{\alpha+1} dx \\ &= \frac{1}{(1 + \frac{\alpha}{2})\pi^{\frac{\alpha}{2}}\lambda_b^{\frac{\alpha}{2}}}. \end{aligned}$$

The pdf of the length of a typical D2D link is

$$f_{L_d}(x) = \begin{cases} \frac{f_D(x)}{\mathbb{P}(D \leq \gamma_I)} = \frac{2\lambda\pi x e^{-\lambda\pi x^2}}{1 - e^{-\lambda\pi\gamma_I^2}} & \text{if } x \in [0, \gamma_I]; \\ 0 & \text{otherwise.} \end{cases}$$

Correspondingly, its α -th moment can be computed as follows:

$$\begin{aligned} \mathbb{E}[L_d^\alpha] &= \int_0^\infty \alpha x^{\alpha-1} \mathbb{P}(L_d \geq x) dx \\ &= \int_0^{\gamma_I} \alpha x^{\alpha-1} \mathbb{P}(L_d \geq x) dx \\ &= \frac{1}{\int_0^{\gamma_I} f_D(x) dx} \int_0^{\gamma_I} \alpha x^{\alpha-1} \int_x^{\gamma_I} f_D(y) dy dx \\ &= \frac{1}{\int_0^{\gamma_I} f_D(x) dx} \cdot \left(\int_0^{\gamma_I} \alpha x^{\alpha-1} \mathbb{P}(D \geq x) dx - \int_0^{\gamma_I} \alpha x^{\alpha-1} \mathbb{P}(D \geq \gamma_I) dx \right), \end{aligned}$$

where $\int_0^{\gamma_I} f_D(x) dx = 1 - e^{-\lambda\pi\gamma_I^2}$, $\int_0^{\gamma_I} \alpha x^{\alpha-1} \mathbb{P}(D \geq \gamma_I) dx = \gamma_I^\alpha e^{-\lambda\pi\gamma_I^2}$ and

$$\begin{aligned} \int_0^{\gamma_I} \alpha x^{\alpha-1} \mathbb{P}(D \geq x) dx &= \int_0^{\gamma_I} \alpha x^{\alpha-1} e^{-\lambda\pi x^2} dx \\ &= \frac{\alpha}{2} (\lambda\pi)^{-\frac{\alpha}{2}} \int_0^{\lambda\pi\gamma_I^2} z^{\frac{\alpha}{2}-1} e^{-z} dz \\ &= \frac{\alpha}{2} (\lambda\pi)^{-\frac{\alpha}{2}} \gamma(\frac{\alpha}{2}, \lambda\pi\gamma_I^2), \end{aligned}$$

where we change variable $z = \lambda\pi x^2$ in the second equality and $\gamma(s, x) = \int_0^x z^{s-1} e^{-z} dz$ is the lower incomplete gamma function. Therefore,

$$\begin{aligned} \mathbb{E}[P_d] &= \mathbb{P}(D \geq \gamma_I) \mathbb{E}[L_c^\alpha] + (1 - \mathbb{P}(D \geq \gamma_I)) \mathbb{E}[L_d^\alpha] \\ &= e^{-\lambda\pi\gamma_I^2} \mathbb{E}[P_c] + (1 - e^{-\lambda\pi\gamma_I^2}) \frac{1}{1 - e^{-\lambda\pi\gamma_I^2}} \\ &\quad \left(\frac{\alpha}{2} (\lambda\pi)^{-\frac{\alpha}{2}} \gamma(\frac{\alpha}{2}, \lambda\pi\gamma_I^2) - \gamma_I^\alpha e^{-\lambda\pi\gamma_I^2} \right) \\ &= e^{-\lambda\pi\gamma_I^2} \mathbb{E}[P_c] + \frac{\alpha}{2} (\lambda\pi)^{-\frac{\alpha}{2}} \gamma(\frac{\alpha}{2}, \lambda\pi\gamma_I^2) - \gamma_I^\alpha e^{-\lambda\pi\gamma_I^2}. \end{aligned}$$

Correspondingly, $\mathbb{E}[\hat{P}_d] = \mathbb{E}[L_d^\alpha]$. To bound $\mathbb{E}[\hat{P}_d]$, we use Alzer's inequality [31]: for all $x \in \mathbb{R}^{++}$

$$(1 - e^{-\tau x^p})^{1/p} < \tau \int_0^x e^{-t^p} dt < (1 - e^{-x^p})^{1/p},$$

where $\tau = 1/\Gamma(1 + 1/p)$, $0 < p < 1$. Using this inequality, we obtain the desired bounds in the proposition statement.

B. Proof of Proposition 2

By definition,

$$\begin{aligned}\mathbb{E}[P_d] &= (1 - \int_{-\infty}^{\gamma_I} f_D(x) dx) \cdot \mathbb{E}[P_c] \\ &+ \int_{-\infty}^{\gamma_I} f_D(x) dx \cdot \int_{-\infty}^{\gamma_I} x^\alpha \frac{f_D(x)}{\int_{-\infty}^{\gamma_I} f_D(x) dx} dx \\ &= (1 - \int_{-\infty}^{\gamma_I} f_D(x) dx) \cdot \mathbb{E}[P_c] + \int_{-\infty}^{\gamma_I} x^\alpha f_D(x) dx.\end{aligned}$$

Taking the derivative of $\mathbb{E}[P_d]$ with respect to γ_I ,

$$\frac{d}{d\gamma_I} \mathbb{E}[P_d] = f_D(\gamma_I)(\gamma_I^\alpha - \mathbb{E}[P_c]).$$

Setting the above derivative to zero, we obtain the stationary point $(\mathbb{E}[P_c])^{1/\alpha}$. It is easy to see that $\mathbb{E}[P_d]$ is decreasing when $\gamma_I \in [0, (\mathbb{E}[P_c])^{1/\alpha}]$ and is increasing when $\gamma_I \in [(\mathbb{E}[P_c])^{1/\alpha}, \infty)$. Hence, $\mathbb{E}[P_d]$ is minimized at $\gamma_I^* = (\mathbb{E}[P_c])^{1/\alpha}$. The proof is complete by plugging the explicit expression for $\mathbb{E}[P_c]$ (given in (2)).

C. Proof of Lemma 1

The derivation follows [26]. To begin with,

$$\mathbb{E}[g(\text{SINR})] = \mathbb{E}[\mathbb{E}[g(\frac{W}{I+N_0/2})|I]], \quad (19)$$

where we condition on I in the last equality. Note

$$\begin{aligned}\mathbb{E}[g(\frac{W}{I+N_0/2})|I] &= \int g(\frac{x}{I+N_0/2}) \sum_{k \in \mathcal{K}} a_k f_{W_k}(x) dx \\ &= \sum_{k \in \mathcal{K}} a_k \int g(\frac{x}{I+N_0/2}) f_{W_k}(x) dx, \quad (20)\end{aligned}$$

where we apply Fubini's Theorem in the last equality. The integral in (20) equals

$$\begin{aligned}& \int_0^\infty g(\frac{x}{I+N_0/2}) \frac{1}{\Gamma(k)\theta_k^k} x^{k-1} e^{-\frac{x}{\theta_k}} dx \\ &= \frac{1}{\Gamma(k)\theta_k^k} (I+N_0/2)^k \int_0^\infty z^{k-1} g(z) e^{-\frac{I+N_0/2}{\theta_k} z} dz, \quad (21)\end{aligned}$$

where we change variable $z = \frac{x}{I+N_0/2}$ in (21). Denoting $f(z) = z^{k-1} g(z)$, applying integration by parts k times, and using the facts $g^{(i)}(z)$ exists and $g^{(i)}(0) < \infty, 0 \leq i \leq k-1$,

$$\begin{aligned}& \int_0^\infty f(z) e^{-\frac{I+N_0/2}{\theta_k} z} dz \\ &= \left(\frac{\theta_k}{I+N_0/2}\right)^k \int_0^\infty f^{(k)}(z) e^{-\frac{I+N_0/2}{\theta_k} z} dz \\ &\quad - \left(\sum_{i=1}^k \left(\frac{\theta_k}{I+N_0/2}\right)^i f^{(i-1)}(z) e^{-\frac{I+N_0/2}{\theta_k} z}\right) \Big|_0^\infty \\ &= \left(\frac{\theta_k}{I+N_0/2}\right)^k \int_0^\infty f^{(k)}(z) e^{-\frac{I+N_0/2}{\theta_k} z} dz \\ &\quad + \left(\frac{\theta_k}{I+N_0/2}\right)^k f^{(k-1)}(0)\end{aligned}$$

$$\begin{aligned}&= \left(\frac{\theta_k}{I+N_0/2}\right)^k \int_0^\infty f^{(k)}(z) e^{-\frac{I+N_0/2}{\theta_k} z} dz \\ &\quad + \left(\frac{\theta_k}{I+N_0/2}\right)^k \Gamma(k) g(0).\end{aligned}$$

Plugging the above equality back into (21),

$$\begin{aligned}& \int g(\frac{x}{I+N_0/2}) f_{W_k}(x) dx \\ &= g(0) + \frac{1}{\Gamma(k)} \int_0^\infty f^{(k)}(z) e^{-\frac{I+N_0/2}{\theta_k} z} dz. \quad (22)\end{aligned}$$

Combining (19), (20) and (22), we have $\mathbb{E}[g(\text{SINR})]$ equals

$$\begin{aligned}& g(0) + \sum_{k \in \mathcal{K}} \frac{a_k}{\Gamma(k)} \int_0^\infty f^{(k)}(z) \mathbb{E}[e^{-\frac{z}{\theta_k} I}] e^{-\frac{N_0/2}{\theta_k} z} dz \\ &= g(0) + \sum_{k \in \mathcal{K}} \frac{a_k}{\Gamma(k)} \int_0^\infty f^{(k)}(z) L_I\left(\frac{z}{\theta_k}\right) e^{-\frac{N_0/2}{\theta_k} z} dz \\ &= g(0) + \sum_{k \in \mathcal{K}} \frac{a_k \theta_k}{\Gamma(k) N_0/2} \int_0^\infty f^{(k)}\left(\frac{\theta_k x}{N_0/2}\right) \mathcal{L}_I\left(\frac{x}{N_0/2}\right) e^{-x} dx,\end{aligned}$$

where $\mathcal{L}_I(s) = \mathbb{E}[e^{-sI}]$ is the Laplace transform of I and we change variable $x = \frac{N_0/2}{\theta_k} z$ in the last equality.

D. Proof of Proposition 3

Consider the conditional Laplace transform

$$\begin{aligned}\mathbb{L}_{I_d}(s) &= \mathbb{E}[e^{-s \sum_{X_i \in \Phi_d \setminus \{o\}} \hat{P}_{d,i} G_i \|X_i\|^{-\alpha}} | \{o\} \in \Phi_d] \\ &= \mathbb{E}^{!o}[e^{-s \sum_{X_i \in \Phi_d} \hat{P}_{d,i} G_i \|X_i\|^{-\alpha}}] \\ &= \mathbb{E}[e^{-s \sum_{X_i \in \Phi_d} \hat{P}_{d,i} G_i \|X_i\|^{-\alpha}}] = e^{-\frac{\pi \lambda_d}{\sin^2(\frac{\alpha}{2})} \mathbb{E}[\hat{P}_d^{\frac{2}{\alpha}}] s^{\frac{2}{\alpha}}},\end{aligned}$$

where $\mathbb{E}^{!o}[\cdot]$ denotes the expectation with respect to the reduced Palm distribution and the third equality follows from Slivnyak's theorem [19]. Note that $\lambda_d = q\lambda(1 - e^{-\lambda\pi\gamma_I^2})$, and from the proof of Prop. 1,

$$\mathbb{E}[\hat{P}_d^{\frac{2}{\alpha}}] = \mathbb{E}[L_d^2] = \frac{1}{\lambda\pi} - \frac{\gamma_I^2 e^{-\lambda\pi\gamma_I^2}}{1 - e^{-\lambda\pi\gamma_I^2}}. \quad (23)$$

Plugging λ_d and $\mathbb{E}[\hat{P}_d^{\frac{2}{\alpha}}]$ into $\mathbb{L}_{I_d}(s)$ yields $\mathbb{L}_{I_d}(s) = e^{-cs\frac{2}{\alpha}}$, where c is given in Prop. 3. The derivation is complete by invoking Eq. (7).

E. Proof of Proposition 6

Note that η^* equals

$$\begin{aligned}& \arg \max_{\eta \in [0,1]} w_c T_c + w_d T_d \\ &= \arg \max_{\eta \in [0,1]} w_c (1 - \eta) Q_c \\ &\quad + w_d (e^{-\lambda\pi\gamma_I^2} (1 - \eta) Q_c + (1 - e^{-\lambda\pi\gamma_I^2}) \eta Q_d) \\ &= \arg \max_{\eta \in [0,1]} \eta \left(w_d (1 - e^{-\lambda\pi\gamma_I^2}) Q_d - w_d e^{-\lambda\pi\gamma_I^2} Q_c - w_c Q_c \right).\end{aligned}$$

This immediately implies that $\eta^* = 1$ if

$$w_d (1 - e^{-\lambda\pi\gamma_I^2}) Q_d \geq w_d e^{-\lambda\pi\gamma_I^2} Q_c + w_c Q_c,$$

and 0 otherwise. The proof is complete by some basic manipulations of the above equality.

F. Proof of Proposition 7

Note that

$$\begin{aligned} & \arg \max_{\eta \in [0,1]} w_c \log T_c + w_d \log T_d \\ &= \arg \max_{\eta \in [0,1]} \log T_c^{w_c} \cdot T_d^{w_d} = \arg \max_{\eta \in [0,1]} g(\eta), \end{aligned}$$

where $g(\eta) = \log(1 - \eta)^{w_c} ((1 - \eta)e^{-\lambda\pi\gamma_i^2} Q_c + \eta(1 - e^{-\lambda\pi\gamma_i^2}) Q_d)^{w_d}$. For ease of notation we let $Q_2 = e^{-\lambda\pi\gamma_i^2} Q_c$ and $Q_3 = (1 - e^{-\lambda\pi\gamma_i^2}) Q_d$. Taking derivative of $g(\eta)$ with respect to η ,

$$\begin{aligned} \frac{d}{d\eta} g(\eta) &= \frac{(1 - \eta)^{w_c - 1} (1 - \eta) Q_2 + \eta Q_3)^{w_d - 1}}{(1 - \eta)^{w_c} ((1 - \eta) Q_2 + \eta Q_3)^{w_d}} (w_c + w_d) \\ &\quad \left((Q_2 - Q_3) \eta - (Q_2 - \frac{w_d}{w_c + w_d} Q_3) \right). \end{aligned} \quad (24)$$

If $Q_2 - Q_3 > 0$, the stationary point $\eta^\dagger = \frac{Q_2 - \frac{w_d}{w_c + w_d} Q_3}{Q_2 - Q_3} = 1 - \frac{w_c}{w_c + w_d} \frac{Q_3}{Q_3 - Q_2} \geq 1$, and $g(\eta)$ monotonically decreases on $\eta \leq \eta^\dagger$ and monotonically increases on $\eta > \eta^\dagger$. Hence, $\eta^* = 0$.

If $Q_2 - Q_3 = 0$, $\frac{d}{d\eta} g(\eta) < 0$ and $g(\eta)$ monotonically decreases. Thus, $\eta^* = 0$.

If $Q_2 - Q_3 < 0$, $g(\eta)$ monotonically increases on $\eta \leq \eta^\dagger$ and monotonically decreases on $\eta > \eta^\dagger$. Note stationary point $\eta^\dagger = 1 - \frac{w_c}{w_c + w_d} \frac{Q_3}{Q_3 - Q_2} < 1$. Hence, $\eta^* = \max(0, \eta^\dagger)$. Also, $\eta^\dagger \leq 0$ if and only if $(w_c + w_d) Q_2 \geq w_d Q_3$, which implies $\eta^* = 0$ if and only if $(w_c + w_d) Q_2 \geq w_d Q_3$.

To sum up,

$$\eta^* = \begin{cases} 1 - \frac{w_c}{w_c + w_d} \frac{Q_3}{Q_3 - Q_2} & \text{if } Q_2 < \frac{w_d}{w_c + w_d} Q_3; \\ 0 & \text{otherwise.} \end{cases}$$

Plugging the explicit expressions of Q_2 and Q_3 complete the proof.

G. Proof of Proposition 8

Denote by

$$\begin{aligned} f_1(\eta) &= -w_c Q_c \cdot \eta + w_c Q_c \\ f_2(\eta) &= -w_d (e^{-\lambda\pi\gamma_i^2} Q_c - (1 - e^{-\lambda\pi\gamma_i^2}) Q_d) \cdot \eta + w_d e^{-\lambda\pi\gamma_i^2} Q_c \end{aligned}$$

By definition $\eta^* = \arg \max_{\eta \in [0,1]} \min(f_1(\eta), f_2(\eta))$. Note that $f_1(\eta)$ is linear on $[0, 1]$ with $f_1(0) = w_c Q_c$ and $f_1(1) = 0$. Also $f_2(\eta)$ is linear on $[0, 1]$ with $f_2(0) = w_d e^{-\lambda\pi\gamma_i^2} Q_c$ and $f_2(1) = w_d (1 - e^{-\lambda\pi\gamma_i^2}) Q_d$.

If $e^{-\lambda\pi\gamma_i^2} Q_c > (1 - e^{-\lambda\pi\gamma_i^2}) Q_d$, both $f_1(\eta)$ and $f_2(\eta)$ decreases on $[0, 1]$. Thus $\eta^* = 0$.

If $e^{-\lambda\pi\gamma_i^2} Q_c \leq (1 - e^{-\lambda\pi\gamma_i^2}) Q_d$ and $f_2(0) > f_1(0)$ (i.e., $w_d e^{-\lambda\pi\gamma_i^2} > w_c$), $f_1(\eta)$ decreases and $f_2(\eta)$ increases on $[0, 1]$ but they do not intersect. In particular, $f_2(\eta) > f_1(\eta), \forall \eta \in [0, 1]$. Thus $\eta^* = 0$.

If $e^{-\lambda\pi\gamma_i^2} Q_c \leq (1 - e^{-\lambda\pi\gamma_i^2}) Q_d$ and $f_2(0) \leq f_1(0)$ (i.e., $w_d e^{-\lambda\pi\gamma_i^2} \leq w_c$), $f_1(\eta)$ decreases and $f_2(\eta)$ increases on $[0, 1]$ and they have a unique intersection. Clearly, the value η^* corresponding to the intersection is the optimal solution to the max-min spectrum partition. Thus, from $f_2(\eta^*) = f_1(\eta^*)$

we have

$$\eta^* = \frac{1}{1 + \frac{1 - e^{-\lambda\pi\gamma_i^2} Q_d}{\frac{w_c}{w_d} - e^{-\lambda\pi\gamma_i^2} Q_c}} \in (0, 1].$$

This completes the proof.

REFERENCES

- [1] M. Corson, R. Laroia, J. Li, V. Park, T. Richardson, and G. Tsirtsis, "Toward proximity-aware internetworking," *IEEE Wireless Communications*, vol. 17, no. 6, pp. 26–33, December 2010.
- [2] 3GPP TR 22.803 V1.0.0, "3rd generation partnership project; technical specification group SA; feasibility study for proximity services (ProSe) (release 12)," Tech. Rep., August 2012.
- [3] K. Doppler, M. Rinne, C. Wijting, C. Ribeiro, and K. Hugl, "Device-to-device communication as an underlay to LTE-advanced networks," *IEEE Communications Magazine*, vol. 47, no. 12, pp. 42–49, December 2009.
- [4] G. Fodor, E. Dahlman, G. Mildh, S. Parkvall, N. Reider, G. Miklós, and Z. Turányi, "Design aspects of network assisted device-to-device communications," *IEEE Communications Magazine*, vol. 50, no. 3, pp. 170–177, March 2012.
- [5] Y.-D. Lin and Y.-C. Hsu, "Multihop cellular: A new architecture for wireless communications," in *Proceedings of IEEE Infocom*, vol. 3, March 2000, pp. 1273–1282.
- [6] H. Wu, C. Qiao, S. De, and O. Tonguz, "Integrated cellular and ad hoc relaying systems: iCAR," *IEEE Journal on Selected Areas in Communications*, vol. 19, no. 10, pp. 2105–2115, October 2001.
- [7] B. Liu, Z. Liu, and D. Towsley, "On the capacity of hybrid wireless networks," in *Proceedings of IEEE Infocom*, vol. 2, 2003, pp. 1543–1552.
- [8] U. C. Kozat and L. Tassiulas, "Throughput capacity of random ad hoc networks with infrastructure support," in *Proceedings of MobiCom*, 2003, pp. 55–65.
- [9] A. Zemplianov and G. de Veciana, "Capacity of ad hoc wireless networks with infrastructure support," *IEEE Journal on Selected Areas in Communications*, vol. 23, no. 3, pp. 657–667, March 2005.
- [10] X. Wu, S. Tavildar, S. Shakkottai, T. Richardson, J. Li, R. Laroia, and A. Jovicic, "FlashlinQ: A synchronous distributed scheduler for peer-to-peer ad hoc networks," in *Proceedings of Allerton*, 2010, pp. 514–521.
- [11] F. Baccelli, N. Khude, R. Laroia, J. Li, T. Richardson, S. Shakkottai, S. Tavildar, and X. Wu, "On the design of device-to-device autonomous discovery," in *Fourth International Conference on Communication Systems and Networks*, 2012, pp. 1–9.
- [12] 3GPP RP-122009, "Study on LTE device to device proximity services," in *3GPP TSG RAN Meeting #58*, December 2012.
- [13] P. Gupta and P. R. Kumar, "The capacity of wireless networks," *IEEE Transactions on Information Theory*, vol. 46, no. 2, pp. 388–404, March 2000.
- [14] A. J. Goldsmith and S. B. Wicker, "Design challenges for energy-constrained ad hoc wireless networks," *IEEE Wireless Communications*, vol. 9, no. 4, pp. 8–27, August 2002.
- [15] A. Ozgur, O. Lévêque, and D. N. Tse, "Hierarchical cooperation achieves optimal capacity scaling in ad hoc networks," *IEEE Transactions on Information Theory*, vol. 53, no. 10, pp. 3549–3572, October 2007.
- [16] S. Weber and J. G. Andrews, "Transmission capacity of wireless networks," *Foundations and Trends in Networking*, vol. 5, no. 2-3, pp. 109–281, 2012.
- [17] S. Xu, H. Wang, T. Chen, Q. Huang, and T. Peng, "Effective interference cancellation scheme for device-to-device communication underlying cellular networks," in *Proceedings of IEEE VTC*, 2010, pp. 1–5.
- [18] C. Yu, K. Doppler, C. Ribeiro, and O. Tirkkonen, "Resource sharing optimization for device-to-device communication underlying cellular networks," *IEEE Transactions on Wireless Communications*, vol. 10, no. 8, pp. 2752–2763, 2011.
- [19] D. Stoyan, W. Kendall, and J. Mecke, *Stochastic Geometry and its Applications*. Wiley New York, 1995.
- [20] J. G. Andrews, F. Baccelli, and R. Ganti, "A tractable approach to coverage and rate in cellular networks," *IEEE Transactions on Communications*, vol. 59, no. 11, pp. 3122–3134, November 2011.
- [21] X. Lin, R. K. Ganti, P. Fleming, and J. G. Andrews, "Towards understanding the fundamentals of mobility in cellular networks," *IEEE Transactions on Wireless Communications*, accepted, January 2013. Available at <http://arxiv.org/abs/1204.3447>.

- [22] F. Baccelli, B. Blaszczyszyn, and P. Muhlethaler, "An Aloha protocol for multihop mobile wireless networks," *IEEE Transactions on Information Theory*, vol. 52, no. 2, pp. 421–436, February 2006.
- [23] M. Haenggi and R. Ganti, "Interference in large wireless networks," *Foundations and Trends in Networking*, vol. 3, no. 2, pp. 127–248, 2009.
- [24] F. Baccelli and B. Blaszczyszyn, "Stochastic geometry and wireless networks - Part I: Theory," *Foundations and Trends in Networking*, vol. 3, no. 3-4, pp. 249–449, 2009.
- [25] T. D. Novlan, H. S. Dhillon, and J. G. Andrews, "Analytical modeling of uplink cellular networks," *IEEE Transactions on Communications*, accepted, January 2013. Available at <http://arxiv.org/abs/1203.1304>.
- [26] K. A. Hamdi, "A useful technique for interference analysis in Nakagami fading," *IEEE Transactions on Communications*, vol. 55, no. 6, pp. 1120–1124, June 2007.
- [27] A. M. Hunter, J. G. Andrews, and S. Weber, "Transmission capacity of ad hoc networks with spatial diversity," *IEEE Transactions on Wireless Communications*, vol. 7, no. 12, pp. 5058–5071, December 2008.
- [28] T. Qin, T. Y. Liu, and H. Li, "A general approximation framework for direct optimization of information retrieval measures," *Information retrieval*, vol. 13, no. 4, pp. 375–397, August 2010.
- [29] X. Lin, J. G. Andrews, and A. Ghosh, "Modeling, analysis and design for carrier aggregation in heterogeneous cellular networks," *submitted to IEEE Transactions on Communications*, November 2012. Available at <http://arxiv.org/abs/1211.4041>.
- [30] J. G. Andrews, "Seven ways that HetNets are a cellular paradigm shift," *IEEE Communications Magazine*, vol. 51, no. 3, pp. 136–144, March 2013.
- [31] H. Alzer, "On some inequalities for the incomplete Gamma function," *Mathematics of Computation*, vol. 66, no. 218, pp. 771–778, April 1997.